Ultrasonics Sonochemistry 78 (2021) 105738

Contents lists available at ScienceDirect

Ultrasonics Sonochemistry

journal homepage: www.elsevier.com/locate/ultson

Ultrasonication promotes extraction of antioxidant peptides from oxhide gelatin by modifying collagen molecule structure

Long He [a], Yongfang Gao [b], Xinyue Wang [a], Ling Han [a], Qunli Yu [a,*], Hongmei Shi [c], Rende Song [d]

[a] College of Food Science and Engineering, Gansu Agricultural University, Lanzhou 730070, China
[b] Laboratory of Agricultural & Food Biomechanics, Institute of Biophysics, College of Science, Northwest A & F University, Yangling, Shaanxi 712100, China
[c] The Institute of Animal Science and Veterinary, Hezuo 747000, China
[d] The Qinghai Work Station of Animal and Veterinary Sciences, Yushu 815000, China

ARTICLE INFO

Keywords:
Ultrasonication
Oxhide gelatin
Antioxidant peptides
Microstructure

ABSTRACT

This study primarily explored the internal mechanism underlying the ultrasonication-induced release of antioxidant peptides. An oxhide gelatin solution was treated ultrasonically (power = 200, 300, and 400 W), followed by enzymatic hydrolysis and structural and morphological analysis. The results showed that ultrasonication increased not only the degree of hydrolysis (DH) and protein recovery rate of the oxhide gelatin but also the ABTS radical scavenging, DPPH radical scavenging, ferrous chelating, and ferric reducing activities of its hydrolysate. The oxhide gelatin hydrolysate treated with 300-W ultrasonication had the maximum antioxidant activities. Ultrasonication inhibited hydrogen bond formation, reduced the crosslinking between collagen molecules, transformed part of the folded structure into a helical structure, and lowered the thermal stability of collagen molecules. The micromorphological analysis revealed that ultrasonication caused the gelatin surface to become loose and develop cracks, and as the power of the ultrasonication increased, the repetition interval distance (dÅ) also increased. Moreover, ultrasonication improved the solubilization, surface hydrophobicity, and interface characteristics and increased the content of basic and aromatic amino acids in the hydrolysate. In conclusion, ultrasonication modifies the protein structure, which increases the enzyme's accessibility to the peptide bonds and further enhances antioxidant peptide release. These findings provide new insights into the application of ultrasonication in the release of antioxidant peptides.

1. Introduction

In recent years, functional foods have become popular worldwide because they provide essential nutrients and have a positive long-term impact on human health, which includes minimizing the risk of chronic diseases [1]. The bioactive compounds in functional foods—including antioxidants, vitamins, natural extracts, and prebiotics—may be beneficial to the nutritional and sensory characteristics of the products. Thus, these products may also represent suitable alternatives or supplements for synthetic drugs [2]. Therefore, further development of these functional foods is essential. Currently, bioactive peptides, especially antioxidant peptides, are considered raw materials for the production of functional foods [3]. Raw materials that can be used to prepare antioxidant peptides are abundant, and its sources include plants, animals, and marine products [4]. However, the content and quality of a protein have a considerable influence on the properties of antioxidant peptides.

Recent studies have suggested that gelatin can be hydrolyzed to produce bioactive peptides. Moreover, the low-molecular-weight (<3-kDa) pepsin hydrolysate of steelhead skin gelatin exhibits dual inhibitory activities against dipeptidyl-peptidase IV and angiotensin-I converting enzyme in vitro [5]. The alkaline protease hydrolysate of squid gelatin was found to cause a twofold increase in the antioxidant capacity of the hydrolysate [6]. The bioactive peptides (<3 kDa) produced from mackerel gelatin have shown the highest antibacterial and antioxidant activities [7]. Oxhide gelatin is a soluble protein mixture produced via partial hydrolysis of cowhide collagen, with an 86.7% protein content and amino acid richness [8]. Therefore, oxhide gelatin may have excellent potential in antioxidant peptide preparation.

Collagen has a triple helix structure stabilized by hydrogen bonds and covalent crosslinkages with other collagen molecules, which limits its applications considerably [9]. The key to obtaining antioxidant

* Corresponding author.
E-mail address: yuqunlihl@163.com (Q. Yu).

https://doi.org/10.1016/j.ultsonch.2021.105738
Received 18 April 2021; Received in revised form 10 August 2021; Accepted 23 August 2021
Available online 31 August 2021

peptides is to break the triple helix structure of collagen and ensure the maximum release of active peptides during hydrolysis. Therefore, finding an effective method to modify collagen structure is essential. Antioxidant peptides are conventionally produced via enzymatic hydrolysis [10]. Moreover, the chemical (acid or base) hydrolysis of collagen is widely used to cleave peptide bonds to produce peptides because it is inexpensive [11]. However, chemical hydrolysis is carried out under extreme temperature and pH conditions, which are not easy to control, and thus the resulting hydrolysate is poor in nutritional quality and low in functionality [12]. Meanwhile, alkali hydrolysis produces lysine, which is unacceptable in foods [11]. Studies have suggested that protein hydrolysates produced via enzymatic hydrolysis are more nutritious than those produced via acid hydrolysis [13]. Therefore, the preparation of bioactive peptides by chemical hydrolysis should be replaced.

Recent studies have suggested using new processing technologies, such as ultrasonication, pulsed electric fields, and high hydrostatic pressures, to produce bioactive peptides [1]. Ultrasonication, an emerging nonthermal processing technology, can produce a cavitation effect in a protein through mechanical vibration and induce conformational changes [14]. Ultrasonic pretreatment of pigskin was found to accelerate the release of acetylcholine esterase inhibitory peptides and enhance the antioxidant activity of fish flavor [15]. In general, ultrasonic pretreatment can increase active compound yield but reduce extraction time and energy [16]. Therefore, ultrasonication may be effective for protein pretreatment to enhance enzymatic hydrolysis of protein. However, information available on the mechanism underlying the ultrasonication-induced antioxidant peptide release from oxhide gelatin is limited.

Therefore, in the current study, we investigated the mechanism underlying the effects of ultrasonic pretreatment on collagen structure and further explored the correlation between the changes in collagen structure and the enzymatic hydrolysis of collagen.

2. Materials and methods

2.1. Materials

Oxhide gelatin was prepared according to the existing method in the laboratory. Alkaline protease was provided from Soleibao Technology (Beijing, China). Diammonium 2,2′-azino-bis (3-ethylbenzothiazoline-6-sulfonate) was purchased from Sigma-Aldrich (St. Louis, MO, USA). Potassium bromide was purchased from Yuanye Biological Technology (Shanghai, China). Furthermore, all the reagents used in this study were analytical grade.

2.2. Ultrasonic treatment of oxhide gelatin

Oxhide gelatin samples were treated using an ultrasonic instrument (SCIENTZ-IID, Ningbo, China). The gelatin powder was dissolved in a 50-mL beaker with deionized water to a concentration of 5% (w/v) and treated for 20 min with ultrasonication at a power of 200, 300, or 400 W. Untreated samples were included in the control group. After treatment, the gelatin solutions were freeze-dried in a lyophilizer (SCIENTZ-18 N/B, Ningbo, China) and subsequently subjected to enzymatic hydrolysis and structural analysis.

2.3. Hydrolysis process

The enzymatic reaction of oxhide gelatin was performed as reported previously [17]. The reaction was carried out under the optimal conditions for alkaline protease (50 °C, pH 8.0). The specific hydrolysis conditions were as follows: alkaline protease, 2 g/L; substrate concentration, 5 g/L; hydrolysis time, 6 h. The enzymatic hydrolysate was obtained and subsequently inactivated in a water bath at 100 °C for 15 min. The obtained solution was divided into two fractions. Of these, one fraction was lyophilized and stored at 4 °C until analysis for DH. The other fraction was centrifuged in an ultrafiltration centrifuge tube with molecular weight cutoff membranes of 3 kDa (UFC901096 Merck Millipore, Shanghai, China) at 6,000 × *g* for 20 min at 4 °C. Thereafter, the < 3-kDa components were lyophilized to determine their antioxidant activities.

2.4. dH

DH of the hydrolyzed oxhide gelatin was determined as described by Zhou et al [18] and calculated as follows:

$$DH(\%) = [(L_t - L_0)/(L_{max} - L_0)] \times 100 \quad (1)$$

where L_t and L_0 are the amount of free amino groups (α-AG) at t min and 0 min, respectively, and L_{max} is the amount of total α-AG in the original homogenate obtained after acid hydrolysis (6 M HCl at 110 °C for 24 h).

2.5. Protein recovery rate

Protein recovery rate was determined as described previously [19]. The hydrolysate protein content was determined with bovine serum albumin as the standard. Protein recovery rate was calculated as follows:

$$\text{Proteinrecoveryrate}(\%) = \frac{\text{Hydrolysateproteincontent}}{\text{Oxhidegelatinproteincontent}} \times 100 \quad (2)$$

2.6. ABTS radical scavenging activity

ABTS solution (14 mM) was mixed with a same volume of 2.45 mM potassium persulfate solution and reacted in the dark at 25 °C for 16 h to prepare ABTS radical reagent solution. This solution was diluted with 25 mM phosphate buffer (pH 6.8) to ensure that the absorbance at 734 nm was 0.75 ± 0.02 as detected on a UV–visible spectrophotometer (T6 New Century; Beijing Puxi General Instrument, China). Subsequently, 25 μL of the hydrolysate was mixed with 3 mL of the ABTS radical reagent solution, followed by incubation at 30 °C for 6 min and absorbance measurement at 734 nm. For blank control, 25 μL of deionized water was used instead of the hydrolysate. The ABTS radical scavenging activity was calculated as follows:

$$\text{ABTSradicalscavengingactivity}(\%) = [(A_b - A)/A_b] \times 100 \quad (3)$$

where A and Ab are the absorbance of the reaction system in the control and treatment group, respectively.

2.7. DPPH radical scavenging activity

The DPPH radical scavenging activity was measured according to the method of Ngo et al [20]. The hydrolysate solution (1 mL) was added to 1 mL of 0.2 mmol/L DPPH in ethanol solution. The mixed solution was left in the dark for 30 min at room temperature, and the absorbance of the samples was measured at 517 nm. The DPPH radical scavenging activity was calculated as follows:

$$\text{DPPHradicalscavenging}(\%) = (1 - \frac{A_S - A_C}{A_b}) \times 100\% \quad (4)$$

where A_s, A_c, and A_b denote the absorbance of the sample–DPPH, sample–ethanol, and DPPH–ethanol solutions, respectively.

2.8. Ferrous chelating activity

The ferrous chelating activity of the hydrolysate was measured as described by Zhang et al [21]. The hydrolysate solution (1 mL) was mixed with distilled water (4.7 mL), followed by incubation with 2 mM $FeCl_2$ (1 mL) and 5 mM ferrozine (200 μL) at 25 °C for 20 min. The absorbance of the samples was measured at 562 nm. The ferrous

chelating activity was calculated as follows:

$$\text{Ferrouschelatingactivity}(\%) = \left(1 - \frac{A_1}{A_C}\right) \times 100 \quad (5)$$

where A_1 and A_c are the absorbance of the sample and control, respectively.

2.9. Ferric reducing activity

The ferric reducing activity of the hydrolysate was determined as described previously [7]. The hydrolysate solution (1 mL) was mixed with 1 mL of 10 mg/mL potassium ferricyanide and then incubated for 20 min at 50 °C. The reaction was stopped by adding 1 mL of 10% trichloroacetic acid and subsequently centrifuged at 3000 × *g* for 10 min at 4 °C. The supernatant (100 μL) was added to 100 μL of distilled water. Subsequently, 20 μL of 1 mg/mL ferric chloride was added to the above mixture and incubated for 10 min at 25 °C. The absorbance of the samples was measured at 700 nm.

2.10. Amino acid analysis

The amino acid composition of the hydrolysate was measured as described by Zou et al [22]. In brief, the samples were hydrolyzed with 6 mol/L HCl in a sealed tube and placed in the oven at 110 °C for 24 h. The total amino acid composition, excluding tryptophan, was determined on an LA8080 automatic amino acid analyzer (Hitachi, Tokyo).

The hydrolysates (1 mL) were mixed with 1 mL of 5-sulfosalicylic acid, followed by centrifugation for 20 min at 10000 × *g* and filtration through a 0.22-μm filter membrane. The supernatant was used for free amino acid (FAA) analysis on the aforementioned amino acid analyzer.

2.11. Fourier transform infrared (FTIR) spectroscopy

The FTIR spectrum was measured with a Fourier transform infrared instrument (Varian 660-IR) as reported previously [23]. In brief, the samples (1 mg) were finely ground with 100 mg of KBr in a mortar and pressed into a disk under a 10-ton/m^2 pressure for 1 min. The spectra were scanned from 500 to 4000 cm^{-1} at a resolution of 4 cm^{-1}.

2.12. X-ray diffraction (XRD) analysis

XRD was performed on an X-ray diffractometer (TD-3700, China) as reported previously [24]. Each sample was scanned from 5° to 50°, with a step of 2θ = 0.02° at 40-kV voltage and 40-mA current.

2.13. Differential scanning calorimetry (DSC)

The thermal properties of ultrasonically treated samples were determined by a differential scanning calorimeter (TA Instruments, New Castle, USA) as described previously [25]. In brief, 10–15 mg of each sample was sealed in an aluminum pan, which was scanned from 15 to 120 °C at a scan rate of 5 °C/min.

2.14. Thermogravimetric analysis (TGA)

TGA of the treated samples was performed by heating the sample from 50 to 600 °C at a heating rate of 25 °C/min. The flow rate of nitrogen, used as the cooling gas, was 10 mL/min.

2.15. Particle size

The ultrasonically treated samples were dissolved in deionized water to a concentration of 1 mg/mL. The particle size and its distribution in the samples were measured in a laser particle size analyzer (Mastersizer 2000, Malvern, UK) at 25 °C.

2.16. Solubility

The solubility of oxhide gelatin samples was measured according to a previously described method [26]. The gelatin powder was dissolved in deionized water to a concentration of 3 mg/mL in a 50-mL beaker and allowed to stand at 4 °C for 60 min. This solution was then centrifuged at 6000 × *g* for 15 min at 4 °C. The supernatant was collected and analyzed for protein concentration by using the Lowry method. Protein solubility (%) was calculated as follows:

$$\text{Proteinsolubility}(\%) = \frac{\text{Proteincontentofthesupernatant}}{\text{Totalproteincontentofthesample}} \times 100 \quad (6)$$

2.17. Surface hydrophobicity

The surface hydrophobicity of the treated samples was measured using 1-anilino-8-naphthalenesulfonate (ANS) according to a previously reported method [27]. Each sample was serially diluted to final concentrations of 0, 0.125, 0.25, 0.5, and 1 mg·mL^{-1}. In total, 1 mL of each diluted sample was mixed with 5 μL of 5 mg/mL ANS. The fluorescence intensity of the sample was measured at an excitation wavelength of 390 nm and emission wavelength of 470 nm on a Perkin Elmer spectrofluorometer (LS 55; Shanghai Simiao Analytical Instrument, Shanghai, China). The initial slope of the plot of sample fluorescence intensity versus sample concentration was regarded as surface hydrophobicity.

2.18. Emulsifying properties

The emulsifying activity index (EAI) and emulsion stability index (ESI) of oxhide gelatin samples were determined as described previously [28]. The oxhide gelatin solution (2 mg/mL) was mixed with soybean oil (4:1, w/v) and homogenized two times at 15,000 r/min for 30 s. Then, 0.06 mL of the emulsion was diluted to 6 mL with 0.1% sodium dodecyl sulfate. The absorbance of the diluted emulsion was recorded at 500 nm immediately (A0) and 30 min after (A_{30}). The EAI and ESI of the samples were calculated using Eqs. (7) and (8), respectively:

$$\text{EAI}\left(\frac{m^2}{g}\right) = \frac{2 \times 2.303 \times A_0 \times N}{C \times \varnothing \times 10^4} \quad (7)$$

where N is the dilution factor, Ø is the volume fraction of soybean oil, and C is the protein concentration (g/mL)

$$\text{ESI}(\text{min}) = \frac{A_0}{A_0 - A_{30}} \times 30 \quad (8)$$

2.19. Foaming properties

The foaming activity index (FAI) and foaming stability index (FSI) of oxhide gelatin samples were determined as described previously [29]. In brief, 15 mL of 1 mg/mL oxhide gelatin solution was placed in a 50-mL beaker and homogenized for 1 min at 10,000 r/min. The volume of the solution was recorded immediately (V_1) and 30 min after (V_2). The FAI and FSI of oxhide gelatin samples were calculated as follows:

$$\text{FAI}(\%) = \frac{V_1 - 15}{15} \times 100\% \quad (9)$$

$$\text{FSI}(\%) = \frac{V_2}{V_1} \times 100\% \quad (10)$$

2.20. Atomic force microscopy (AFM)

The morphology of the treated samples was determined as described previously [30]. A drop of a sample (2 μg/mL) was placed on a newly cut mica sheet and dried at room temperature for 2 h. The samples were tested in the AFM tapping mode with a silicon cantilever probe (5 N/M),

and each image was analyzed using Nanoscope Analysis at three different regions.

2.21. Scanning electron microscopy (SEM)

The treated sample powders were placed in a vacuum drying chamber. A metal film was subsequently sputter-coated on the surface of the sample using a sputter coater at 10 kV, and the structure was amplified 300 times.

2.22. Statistical analysis

Each experiment was performed in triplicate. Statistical analysis was performed using SPSS (version 20.0; SPSS, Chicago, IL, USA) to determine the differences and their significance. The differences between the mean values were compared by Duncan's new multiple range test ($P < 0.05$). Origin (version 9.0) was employed for plotting the graphs and analyzing the dynamics.

3. Results and discussion

3.1. Ultrasonication promotes antioxidant activity in oxhide gelatin hydrolysates

The effects of ultrasonic pretreatment (200, 300, and 400 W) on the hydrolysis properties (i.e., DH and protein recovery rate) of oxhide gelatin and the ABTS radical scavenging activities of the hydrolysate are shown in Fig. 1. The DH of oxhide gelatin increased with as the ultrasonication power increased. It significantly increased at 200–300 W ($P < 0.05$) but became nonsignificant at 300–400 W. In other words, the increase in the ultrasonication power promoted oxhide gelatin hydrolysis. These results agree with those of Vidal et al [31], who noted considerable increases in DH after ultrasonication and proposed that this phenomenon may be due to the ultrasonication-induced structural changes in gelatin.

In the protein hydrolysis process, the greater the protein recovery rate, the better is the hydrolysis effect [32]. Compared with the control group, the protein recovery rate of the hydrolysates were significantly higher after ultrasonication of 200–300 W, but no significant changes was observed when the ultrasonic power was increased further. In terms of energy consumption, the ultrasonic power of 300 W is more conducive to protein hydrolysis. These results showed that the uptrend in the protein recovery rate was consistent with the uptrend in DH. The DH was also closely related to the protein recovery rate.

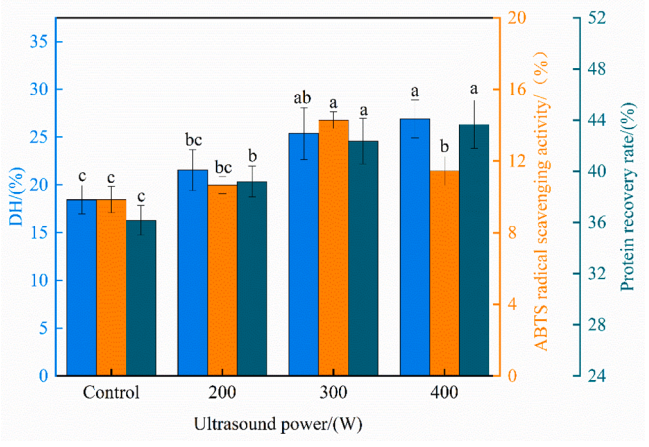

Fig. 1. The degree of hydrolysis (DH) and protein recovery rate of oxhide gelatin and the ABTS radical scavenging activity of the hydrolysate. Different lowercase letters represent significant differences at $P < 0.05$. Error bars indicate the standard errors of the mean.

The FAA content may reflect the hydrolysis process of proteins [33]. As shown in Table 1, the FAA content in the oxhide gelatin hydrolysate pretreated with ultrasonication at 200 W was 0.864 g/100 g, which was 5.9% higher than that in the control (0.816 g/100 g). The FAA content was increased with the further enlargement of ultrasonic power—consistent with the DH and protein recovery rate results.

The results also showed that the ABTS radical scavenging activity of the hydrolysate reached the maximum value of 14.29% at 300 W, which was 45.20% higher than that of the control—possibly because ultrasonication modified the protein structure and increased basic and aromatic amino acid contents in the hydrolysate. As shown in Table 2, 300-W ultrasonication pretreatment increased the total basic amino acid content in the oxhide gelatin hydrolysate by 10.94%. These results are similar to those of Zou et al. [22], who observed that porcine cerebral hydrolysate pretreated with ultrasonication contained high basic amino acid content. Notably, basic amino acids (Lys, Arg, and His) can be used as hydrogen donors and have a strong free radical scavenging activity [22]. Aromatic amino acids are also considered effective free radical scavengers, possibly because of the special structure of their phenolic groups [34]. In the present study, the Asp and Glu contents in the hydrolysate of oxhide gelatin pretreated with 300-W ultrasonication were 5 and 8.66 g/100 g, respectively; these values were 7.06% and 6.78% higher than those in the control (4.67 and 8.11 g/100 g, respectively). In addition, the antioxidant capacity of the hydrolysate was related to the content of the C-terminal amino acids (Arg and Tyr) and the N-terminal amino acids (His, Phe, and Leu) [34]. Compared with the control, the 300-W ultrasonication–treated oxhide gelatin hydrolysate had 22.69% and 28.74% higher the C-terminal and N-terminal amino acid contents, respectively. The results for ABTS radical scavenging activity also corresponded well with the results for DH, indicating that the increase in

Table 1
Effects of ultrasound on the free amino acids content in the hydrolysate (g/100 g).

Free amino acids	Control	200 W	300 W	400 W
Asp	0.0081 ± 0.0002^{b}	0.0087 ± 0.0003^{a}	0.0084 ± 0.0003^{ab}	0.0084 ± 0.0002^{ab}
Thr	0.0019 ± 0.0003	0.002 ± 0.0006	0.002 ± 0.002	0.002 ± 0.0004
Ser	0.013 ± 0.002	0.013 ± 0.003	0.013 ± 0.002	0.013 ± 0.003
Glu	0.0041 ± 0.0002^{b}	0.0047 ± 0.0003^{a}	0.0042 ± 0.0004^{b}	0.004 ± 0.0002^{b}
Gly	0.054 ± 0.004	0.056 ± 0.002	0.055 ± 0.003	0.057 ± 0.004
Ala	0.015 ± 0.002	0.015 ± 0.002	0.015 ± 0.003	0.015 ± 0.002
Cys	nd	nd	nd	nd
Val	0.002 ± 0.0006	0.002 ± 0.0006	0.0019 ± 0.0002	0.0021 ± 0.0002
Met	0.0024 ± 0.0003	0.0024 ± 0.0004	0.0024 ± 0.0003	0.0025 ± 0.0003
Iie	nd	nd	nd	nd
Leu	nd	nd	nd	nd
Tyr	0.68 ± 0.02^{b}	0.72 ± 0.03^{ab}	0.73 ± 0.025^{a}	0.77 ± 0.025^{a}
Phe	nd	nd	nd	nd
Lys	0.0063 ± 0.0008	0.0067 ± 0.0003	0.0063 ± 0.0005	0.0071 ± 0.0003
His	0.0079 ± 0.0003^{bc}	0.0077 ± 0.0008^{c}	0.0088 ± 0.0004^{ab}	0.0089 ± 0.0003^{a}
Arg	0.011 ± 0.001	0.012 ± 0.002	0.01 ± 0.004	0.012 ± 0.003
Pro	0.013 ± 0.002	0.014 ± 0.002	0.014 ± 0.003	0.014 ± 0.003
TAA	0.816 ± 0.017^{b}	0.864 ± 0.025^{ab}	0.876 ± 0.03^{a}	0.913 ± 0.03^{a}

Different letters in the same row indicate significant differences ($P < 0.05$). No letters in the same row indicate no significant differences ($P > 0.05$). nd: not detected. FAA: the content of total free amino acids.

Table 2
Effects of ultrasound on the amino acids content in the hydrolysate (g/100 g).

Amino acids	Control	200 W	300 W	400 W
Asp	4.67 ± 0.33	4.95 ± 0.19	5 ± 0.35	4.87 ± 0.41
Thr	1.46 ± 0.06	1.56 ± 0.17	1.56 ± 0.19	1.54 ± 0.16
Ser	2.53 ± 0.15	2.67 ± 0.18	2.7 ± 0.26	2.65 ± 0.18
Glu	8.11 ± 0.16^{b}	8.54 ± 0.16^{a}	8.66 ± 0.17^{a}	8.46 ± 0.16^{a}
Gly	19.08 ± 1.28	20.32 ± 0.83	20.6 ± 1.6	20.13 ± 1.15
Ala	6.69 ± 0.31^{b}	7.27 ± 0.18^{a}	7.32 ± 0.17^{a}	7.12 ± 0.15^{a}
Cys	nd	nd	nd	nd
Val	1.79 ± 0.03	1.96 ± 0.15	1.98 ± 0.16	1.92 ± 0.14
Met	0.34 ± 0.04^{b}	0.6 ± 0.1^{a}	0.6 ± 0.05^{a}	0.59 ± 0.09^{a}
Iie	0.95 ± 0.08	1.15 ± 0.14	1.15 ± 0.1	1.17 ± 0.25
Leu	2.41 ± 0.07^{b}	2.64 ± 0.21^{a}	2.92 ± 0.15^{a}	2.59 ± 0.12^{a}
Tyr	0.57 ± 0.12c	0.79 ± 0.06b	1.4 ± 0.13a	0.74 ± 0.07bc
Phe	1.47 ± 0.17^{b}	1.75 ± 0.17^{ab}	2.1 ± 0.35^{a}	1.88 ± 0.25^{ab}
Lys	2.76 ± 0.18	2.98 ± 0.19	3.02 ± 0.22	2.95 ± 0.21
His	0.47 ± 0.05	0.57 ± 0.09	0.58 ± 0.08	0.53 ± 0.11
Arg	5.82 ± 0.5	6.30 ± 1.10	6.44 ± 0.13	6.22 ± 0.69
Pro	9.79 ± 0.79	10.57 ± 0.85	10.7 ± 0.55	10.47 ± 0.49
TAA	68.93 ± 4.3^{b}	76.43 ± 4.3^{ab}	76.73 ± 4.62^{a}	73.83 ± 4.59^{ab}

Different letters in the same row indicate significant differences ($P < 0.05$). No letters in the same row indicate no significant differences ($P > 0.05$). nd: not detected. TAA: the content of total amino acids.

ABTS radical scavenging activity may be related to the increase in DH. Our results for ABTS radical scavenging activity also agreed with those of Kangsanant, Murkovic, and Thongraung [35], who found a positive correlation between DH and antioxidant activity. As shown in Fig. 2, the DPPH radical scavenging, ferrous chelating, and ferric reducing activities of the 300-W ultrasonication–treated hydrolysate were 64.10%, 57.75%, and 11.3% higher than those of the control, respectively (all $P < 0.05$). Similar results have been reported for goose-liver, soy, and arrowhead proteins pretreated with ultrasonication [36–38]. The possible reason underlying this phenomenon is that the changes in the collagen conformation and bioactive peptide release from oxhide gelatin were further enhanced by the ultrasonic pretreatment. However, the antioxidant properties of the hydrolysis of oxhide gelatin decreased when the ultrasonic power was increased to 400 W ($P < 0.05$). Similar results have been reported in goose liver protein treated using ultrasonication at different powers [22]: the DPPH radical scavenging rate, ferrous chelating, and hydroxyl radical scavenging activity of goose liver protein hydrolysate were higher after 300-W ultrasonic treatment than after 600-W ultrasonic treatment. Rice bran proteins treated with ultrasonication (power: 50, 100, and 150 W; time: 10, 25, and 40 min) also demonstrated similar trends [39]: The DPPH radical scavenging rate of bioactive peptides reached the highest after 50-W ultrasonication

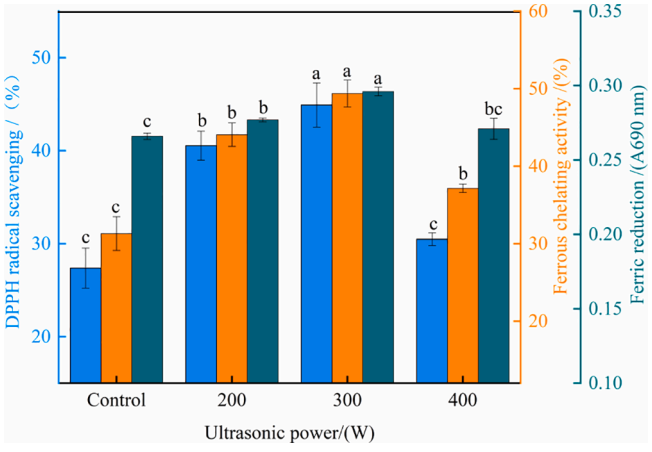

Fig. 2. The DPPH radical scavenging, ferrous chelating, and ferric reducing activity of the hydrolysate. Different lowercase letters represent significant differences at $P < 0.05$. Error bars indicate the standard errors of the mean.

for 10 min, and it was closely related to the DH of the protein. These results contrasted the results for basic and aromatic amino acid contents, which demonstrated nonsignificant differences between the 300 and 400 W ultrasonic treatments. Therefore, in the current study, the 300-W ultrasonication–treated hydrolysate showed the highest DPPH radical scavenging rate and ABTS radical scavenging activity. This result was associated not only with the specific amino acid contents but also with the collagen structure of the oxhide gelatin, as indicated by the low number of internal hydrogen bond—which possibly affected the protein peptide chains and thus led to antioxidant substance release.

3.2. Ultrasonication facilitates protein structure unfolding and weakens protein–protein interaction

To explore the mechanism underlying the improvement in antioxidant capacity of the enzymatic hydrolysis products from ultrasonication-pretreated oxhide gelatin, we focused on the FTIR spectroscopy on the samples (Fig. 3A). The results demonstrated the amide A peak in the control, 200 W, 300 W, and 400 W sample at 3270.68, 3283.215, 3307, and 3270.91 cm^{-1}, respectively. Generally, the amide A band appears at 3400–3440 cm^{-1}. However, when the N–H group forms a hydrogen bond, it may become transferred to a lower wavenumber. In the present study, the samples pretreated with 300-W ultrasonication had the fewer hydrogen bonds and the lower stability compared with the control. The peak value of amide B—related to the asymmetric stretching of CH_2 [26]—in the control and treatment groups was about 2922 cm^{-1}; nevertheless, the amplitude of the amide B bands in the treated groups was lower than that in the control group, but no significant changes in amplitude of the amide B band were observed in the treated groups. The amide I peak is mainly related to the stretching vibration of the carbonyl group. Compared with the control group, the treated groups had a lower wavenumber and a higher amplitude for the amide I peak, indicating that ultrasonication weakened the crosslinking between protein molecules. Next, the spectrum between 1600 and 1700 cm^{-1} was deconvoluted, and the Gaussian function was used to fit the spectrum to calculate the relative content of the secondary structure—as shown in Fig. 3B. The results showed that α-helix contents increased by 10.59%, the random coil disappeared, and the β-turn contents remained unchanged in the treated groups compared with the control group—indicating that ultrasonication transformed partially folded conformation be into a helical structure. This was possible because of the thermal uncoupling effect and the aggregation between the reactive groups (C═O) of unfold α-chain induced by ultrasonication [40]. Moreover, the amide II and II absorbance peaks—related to NH bending vibrations, CN stretching vibration, and CH stretching [23]—in the control and treated groups were at similar positions, at 1540 and 1236 cm^{-1}, respectively.

The broad peak at approximately $2\theta = 21^{\circ}$ in the XRD pattern may be related to the diffuse scattering from the multiscaled collagen structure. Moreover, the method of Zhu et al [41] may be used to calculate the repeat spacing distance (dÅ). In general, the smaller the dÅ, the more compact is the structure. As shown in Fig. 4A, the changes of dÅ between the control and 200-W ultrasonication groups were nonsignificant. However, when the ultrasonication power exceeded 200 W, dÅ increased—indicating loose protein structure formation, possibly because ultrasonication treatment weakened the interaction between collagen molecules [42]. The aforementioned results are consistent with our SEM results (Fig. 6A3–D3).

3.3. Ultrasonication changes protein particle morphology

To explore the nanoscale morphology of the collagen molecules, we used AFM. As shown in Fig. 9, the topography of collagen molecules was circular and nano-sized (diameter in control = 150–170 nm). Under different ultrasonication powers of 200, 300, and 400 W, the diameter ranges were 60–80, 70–80, and 35–60 nm, respectively. The diameter of 400 W ultrasonication–treated oxhide gelatin was only 1/4 to 1/3 that of

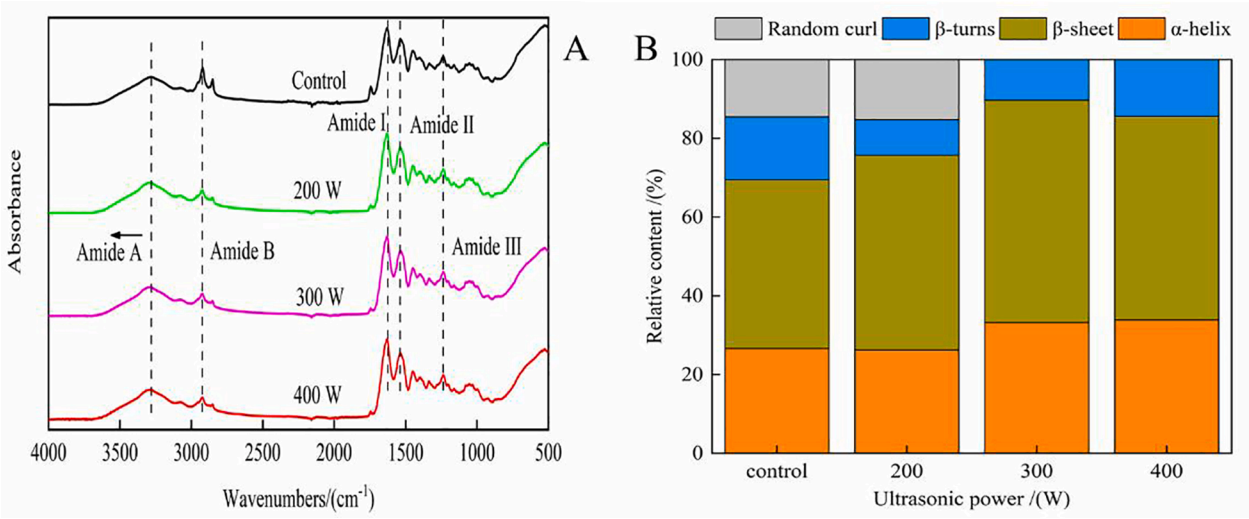

Fig. 3. Fourier transform infrared spectra (A) and relative content of secondary structure (B) of collagen molecules in oxhide gelatin.

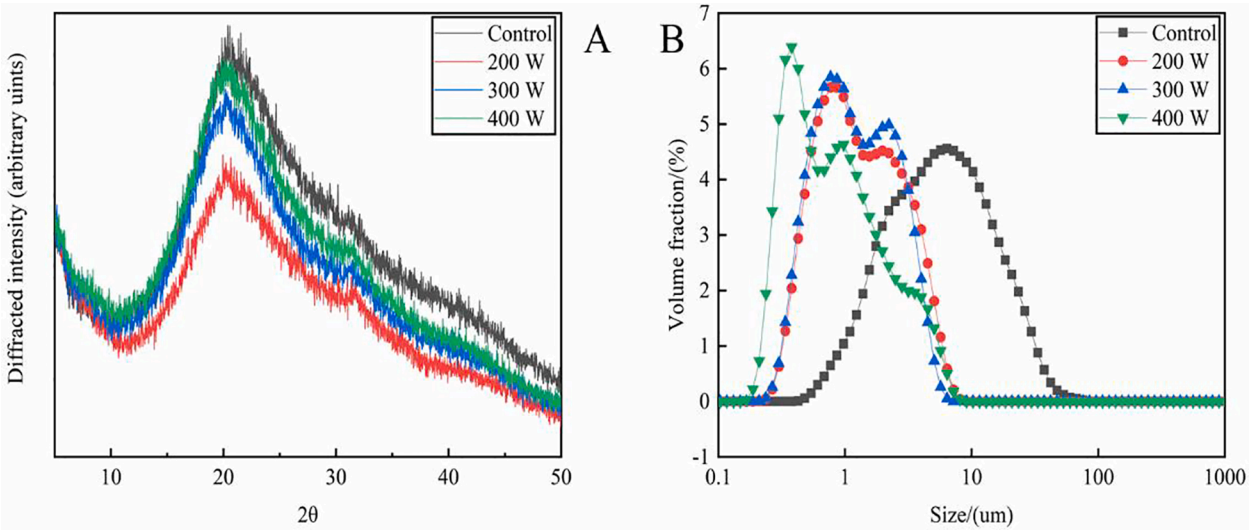

Fig. 4. The patterns of XRD (A) and particle size (B) of oxhide gelatin.

the control oxhide gelatin. This finding corresponds well with that of Zhou et al [18], who indicated that ultrasonication changed surface topography and distribution of corn gluten meal particles, enhancing the enzymolysis rate. Moreover, the collagen molecule nanoparticle dispersion became relatively more uniform after 400-W ultrasonication.

The microstructures of the control and treated proteins were examined via SEM (Fig. 10). The oxhide gelatin surface in the ultrasonic treatment group was incompact and showed cracks, especially as the ultrasonic power increased—consistent with the observations of AFM. The reason for these results was that the shear force was generated when the polymer chain was broken through ultrasonication [43].

3.4. Ultrasonication promotes protein solubility

Ultrasonication breaks down protein aggregates into small particles and improves protein solubility [28]. The current results showed that solubility significantly increased after 0–400-W ultrasonication ($P < 0.05$) but became nonsignificant after 200–300-W ultrasonication. The solubility of at 200-W ultrasonication–treated samples was 75.88, which was 26.4% higher than that of the control (Fig. 5)—possibly because of the shear and cavitation produced by ultrasonication, which promoted the solvent infiltration rate. Similar results have been reported for other proteins, such as egg-white, rice, and pea proteins [33,44].

3.5. Ultrasonication increases number of hydrophobic groups on protein surface

Protein surface hydrophobicity (H0) indicates the degree of protein unfolding and is determined based on the contents of hydrophobic residues, such as leucine and alanine [45]. H0 of the treated groups was higher than that of the control group, with the maximum value being reached with 300-W ultrasonication (Fig. 5). The results were consistent with those of Cuevas-Acuña et al [46], who found that the H0 of tilapia skin gelatin increased after ultrasonication. The reason for this phenomenon was that ultrasonication induced the cleavage of noncovalent bonds, leading to polypeptide chain unfolding and hydrophobic residue exposure [47].

3.6. Ultrasonication improves protein interface properties

EAI indicates the interfacial area stabilized by per unit weight of protein [48]. As shown in Fig. 6, the EAI of oxhide gelatin samples

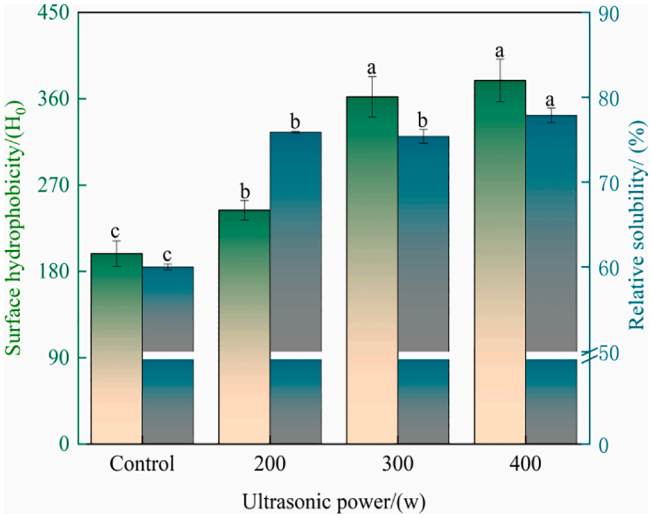

Fig. 5. The surface hydrophobicity and relative solubility of oxhide gelatin. Different lowercase letters represent significant differences at $P < 0.05$. Error bars indicate the standard errors of the mean.

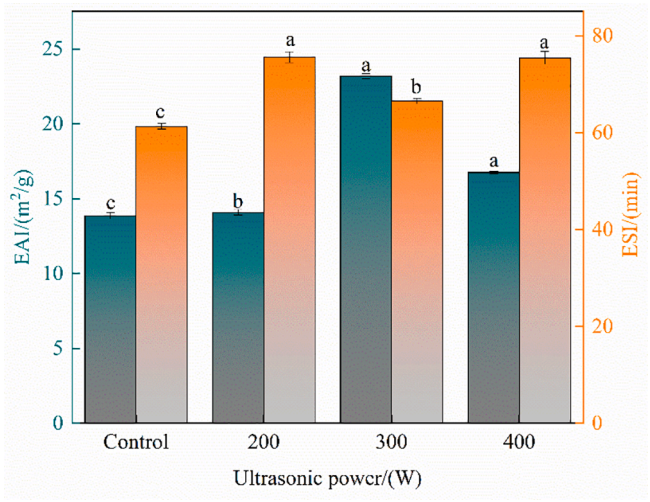

Fig. 6. The emulsion activity index (EAI) and emulsion stability index (ESI) of oxhide gelatin samples. Different lowercase letters represent significant differences at $P < 0.05$. Error bars indicate the standard errors of the mean.

increased after 0–400-W ultrasonication ($P < 0.05$) and peaked with 300-W ultrasonication—indicating that 300-W ultrasonication improved the migration ability of oxhide gelatin from water to the oil–water interface. The results were consistent with those of Akram and Zhang [48], who found that the EAI increased after ultrasonication.

Moreover, he ESI of the oxhide gelatin samples increased after ultrasonication ($P < 0.05$), indicating that ultrasonication improved the hydrophobicity of proteins and their ability to remain at the oil–water interface. This finding corresponds well with that of Zou et al. [49], who found that ultrasonication enhanced the ESIs of sarcoplasmic, millet, and quinoa-seed proteins. Notably, the ESI of oxhide gelatin samples decreased significantly at 300 W, possibly the reduced particle size and enhanced solubility caused by ultrasonication accelerated the protein diffusion rate [50].

The FAI indicates the ability of proteins to migrate, adsorb, and reorient at the air–water interface [51]. The FAI in the treated groups was higher than that in the control, and its value was the maximum for 300-W ultrasonication (Fig. 7). The results indicated that the ultrasonication promoted the oxhide gelatin to produce a sufficient number

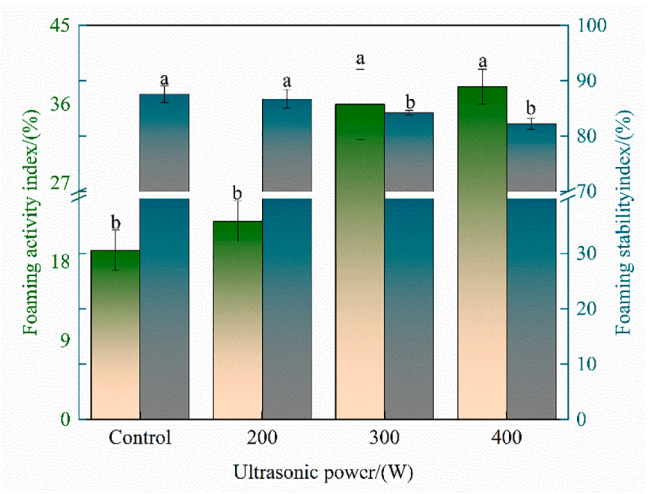

Fig. 7. The foaming activity index (FAI) and foaming stability (FSI) of oxhide gelatin samples. Different lowercase letters represent significant differences at $P < 0.05$. Error bars indicate the standard errors of the mean.

of hydrophobic patches to quickly migrate to the air–water interface. After ultrasonication, the oxhide gelatin particles were more evenly dispersed in the solution, which may have increased the FAI [52].

Moreover, the FSI of the treated samples was lower than that of the controls—but without significant changes for 0–200-W ultrasonication. The results were consistent with those of Tang, Du, and Fu. [29], who found that the FSI of the Moringa *oleifera* seed protein decreased after ultrasonication. The possible reason for this phenomenon is that ultrasonication increased the relative content of soluble collagen.

3.7. Ultrasonication lowers protein denaturation temperature

In collagen, thermal stability differences are correlated with structure diversification [48]. The changes in DSC thermograms in our control and treated group are presented in Fig. 8A. The peak temperature in the DSC thermograms is an extremely important parameter, which reflects protein denaturation temperature. The denaturation temperature of the sample in the treated groups was lower than that in the control group, and it decreased as the ultrasonication power increased. These results are consistent with those of Mir, Riar, and Singh [53], who found that the denaturation temperature of Album seed protein isolates lowered after ultrasonication. The energy required to induce protein denaturation is expressed as denaturation enthalpy (ΔH). The denaturation ΔH of collagen decreased significantly after ultrasonication, especially when ultrasonication power was > 300 W. The reason for this phenomenon was that ultrasonication caused changes in protein structure and conformation.

3.8. Ultrasonication accelerates protein thermal degradation

TGA provides the functions of weight percentage and temperature, whereas. differential thermal analysis (DTA) indicates weight percentage and temperature derivatives. Our TGA and DTA are illustrated in Fig. 8B. In general, the trend of weight loss in the control was similar to that in the treated groups. The thermal degradation process of gelatin can be divided into three stages: the first stage is at 100–200 °C, which is mainly due to bound water evaporation and separation; the second is at 200 ~ 500 °C, where the weight loss is mainly due to the degradation of the molecular chain in protein; and the third stage is at 500–600 °C, where the degradation completes and weight becomes stable. The temperature of severe thermal degradation was smaller in the treated groups than that in the control group, and it decreased as the ultrasonication power increased—indicating that ultrasonication accelerates

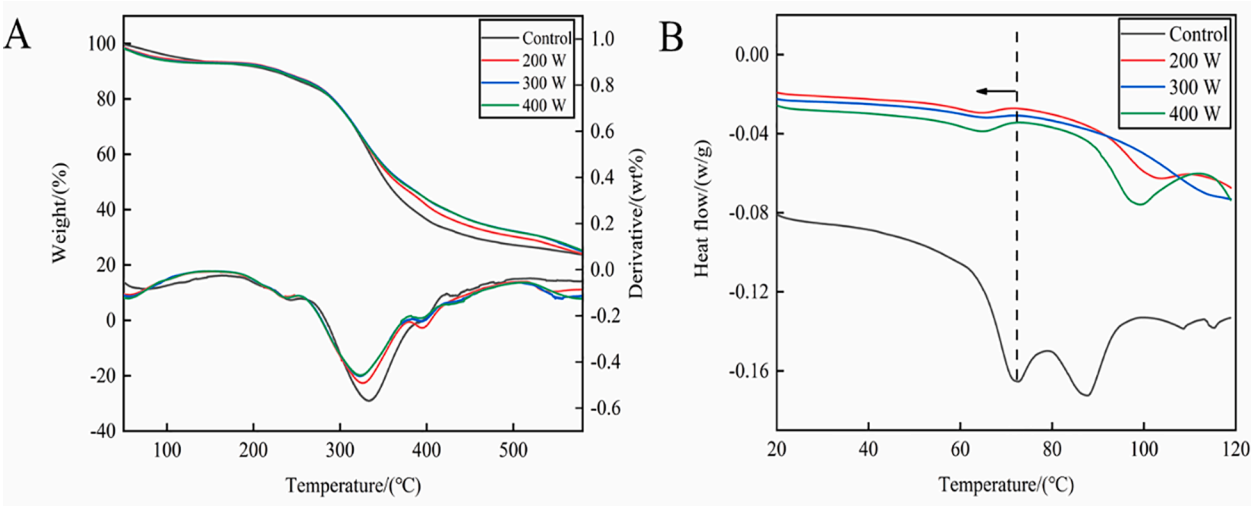

Fig. 8. Differential scanning calorimetry (DSC) (A) and thermo-gravimetric analysis (TGA)/differential thermal analysis (DTA) (B) of collagen molecules in oxhide gelatin.

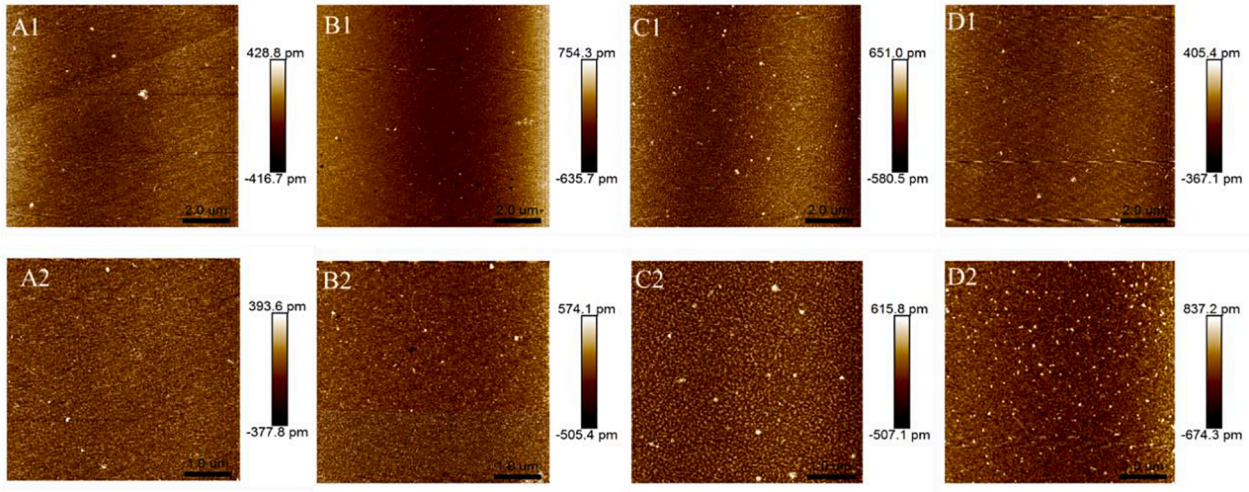

Fig. 9. AFM analysis for the oxhide gelatin samples in the control (A1–A2) and treated groups (B1–B2, C1–C2, D1–D2). B1–B2, C1–C2 and D1–D2 represent the ultrasonic processing time of 200 W, 300 W and 400 W, respectively. Scale bar: 10 μm (A1, B1, C1, and D1), 5 μm (A2, B2, C2, and D2).

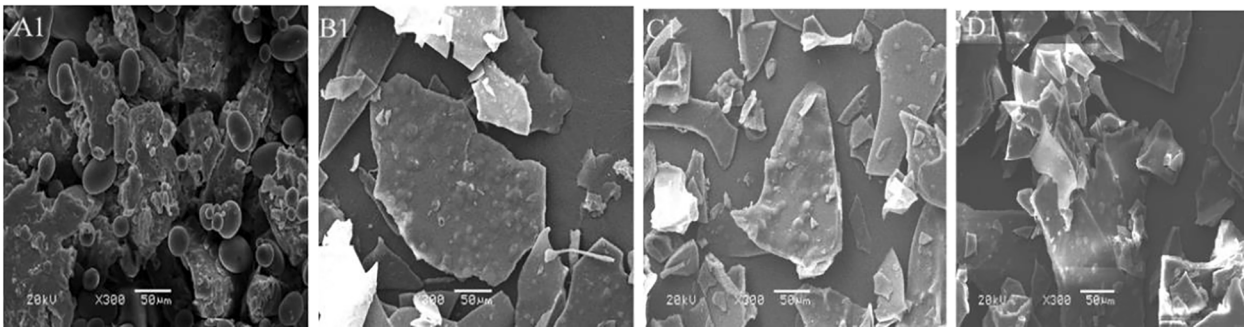

Fig. 10. SEM images of the oxhide gelatin samples in the control (A) and treated groups (B1–D1). B1, C1 and D1 represent the ultrasonic processing time of 200 W, 300 W and 400 W, respectively.

the thermal degradation of oxhide gelatin and reduces protein thermal stability. These results are consistent with those of Mir, Riar, and Singh [53], who found that the thermal stability of the Album protein isolates decreased after ultrasonication. The mechanism underlying this phenomenon is protein breakdown caused by cavitation and turbulence [54].

3.9. Ultrasonication promotes particle size reduction

As shown in Fig. 4B, the average particle sizes of the 0-, 200-, 300-,

and 400-W ultrasonication–treated samples were 6410, 865, 769, and 768 nm, respectively. The particle sizes of the sample were smaller in the treated groups than in the control group, and they decreased further as the ultrasonication power increased. These results are consistent with those of Nasrollahzadeh et al [55], who found that ultrasonication loosened the soybean protein isolate structure and reduced its average particle size. This phenomenon occurred because the strong cavitation effect due to ultrasonication reduced collagen molecule particle size [46]. However, the differences in the average particle sizes between 200- and 300-W ultrasonication–treated samples were nonsignificant, and the size was the smallest in the 400-W ultrasonication–treated sample. These results are consistent with those for DH in our study. Therefore, we believe that an ultrasonication power of 300 W is the most suitable for antioxidant peptide extraction from oxhide gelatin because it provides the most efficient protein modification with the least energy consumption.

4. Conclusion

In summary, the DH and protein recovery rate of oxhide gelatin and the antioxidant activity of the hydrolysate increases after ultrasonication. Ultrasonication inhibits hydrogen bond formation, reduces the crosslinking between collagen molecules, transforms part of the folded structure into a helical structure, and reduces the thermal stability in collagen molecules. The gelatin surface becomes loose and shows cracks after ultrasonication, and the dÅ increases as the ultrasonication power increases. Moreover, ultrasonication improves the solubilization, surface hydrophobicity, and interface characteristics as well as increases basic and aromatic amino acid contents in the hydrolysate. In conclusion, by modifying the protein structure, ultrasonication increases the accessibility of an enzyme to the peptide bonds of the protein and thus enhances the release of antioxidant peptides further.

CRediT authorship contribution statement

Long He: Data curation, Investigation, Methodology, Writing – original draft. **Yongfang Gao:** Validation, Supervision. **Xinyue Wang:** Software, Visualization. **Ling Han:** Writing – review & editing. **Qunli Yu:** Project administration, Resources. **Hongmei Shi:** Conceptualization, Supervision. **Rende Song:** Formal analysis.

Declaration of Competing Interest

The authors declare that they have no known competing financial interests or personal relationships that could have appeared to influence the work reported in this paper.

Acknowledgments

This work was supported by the ecological beef and mutton cascade processing and industrialization (grant number 2020C-18) and Agriculture Research System of China (grant number CARS-37). We thank the editor and referees for their valuable comments and suggestions on an earlier draft of this manuscript.

References

[1] C. Ozuna, I. Paniagua-Martínez, E. Castaño-Tostado, L. Ozimek, S.L. Amaya-Llano, Innovative applications of high-intensity ultrasound in the development of functional food ingredients: production of protein hydrolysates and bioactive peptides, Food Res. Int. 77 (2015) 685–696.
[2] S. Misra, P. Pandey, H.N. Mishra, Novel approaches for co-encapsulation of probiotic bacteria with bioactive compounds, their health benefits and functional food product development: a review, Trends Food Sci. Technol. 109 (2021) 340–351.
[3] B. Cakir, T. Tunali-Akbay, Potential anticarcinogenic effect of goat milk-derived bioactive peptides on HCT-116 human colorectal carcinoma cell line, Anal. Biochem. 622 (2021), 114166.
[4] S.A. Tadesse, S.A. Emire, Production and processing of antioxidant bioactive peptides: a driving force for the functional food market, Heliyon 6 (2020), e04765.
[5] I.W.Y. Cheung, E.C.Y. Li-Chan, Enzymatic production of protein hydrolysates from steelhead (Oncorhynchus mykiss) skin gelatin as inhibitors of dipeptidyl-peptidase IV and angiotensin-I converting enzyme, J. Funct. Foods 28 (2017) 254–264.
[6] A. Alemán, B. Giménez, P. Montero, M.C. Gómez-Guillén, Antioxidant activity of several marine skin gelatins, LWT – Food Sci. Technol. 44 (2011) 407–413.
[7] A. Mirzapour-Kouhdasht, M. Moosavi-Nasab, Y.-M. Kim, J.-B. Eun, Antioxidant mechanism, antibacterial activity, and functional characterization of peptide fractions obtained from barred mackerel gelatin with a focus on application in carbonated beverages, Food Chem. 342 (2021), 128339.
[8] L. He, Y. Gao, L. Han, Q. Yu, R. Zang, Enhanced gelling performance of oxhide gelatin prepared from cowhide scrap by high pressure-assisted extraction, J. Food Sci. 86 (2021) 2525–2538.
[9] S.M. Nuñez, F. Guzmán, P. Valencia, S. Almonacid, C. Cárdenas, Collagen as a source of bioactive peptides: A bioinformatics approach, Electron. J. Biotechnol. 48 (2020) 101–108.
[10] L. Wang, M. Ma, Z. Yu, S.-K. Du, Preparation and identification of antioxidant peptides from cottonseed proteins, Food Chem. 352 (2021), 129399.
[11] S.K. Ulug, F. Jahandideh, J. Wu, Novel technologies for the production of bioactive peptides, Trends Food Sci. Technol. 108 (2021) 27–39.
[12] H.G. Kristinsson, B.A. Rasco, Biochemical and Functional Properties of Atlantic Salmon (Salmo salar) Muscle Proteins Hydrolyzed with Various Alkaline Proteases, J. Agric. Food. Chem. 48 (2000) 657–666.
[13] N. Wisuthiphaet, S. Klinchan, S. Kongruang, Fish Protein Hydrolysate Production by Acid and Enzymatic Hydrolysis (2016).
[14] N. Al-Ruwaih, J. Ahmed, M.F. Mulla, Y.A. Arfat, High-pressure assisted enzymatic proteolysis of kidney beans protein isolates and characterization of hydrolysates by functional, structural, rheological and antioxidant properties, LWT 100 (2019) 231–236.
[15] F.B. Siewe, T.G. Kudre, B.K. Bettadaiah, B. Narayan, Effects of ultrasound-assisted heating on aroma profile, peptide structure, peptide molecular weight, antioxidant activities and sensory characteristics of natural fish flavouring, Ultrason. Sonochem. 65 (2020), 105055.
[16] C. Wen, J. Zhang, J. Zhou, Y. Duan, H. Zhang, H. Ma, Effects of slit divergent ultrasound and enzymatic treatment on the structure and antioxidant activity of arrowhead protein, Ultrason. Sonochem. 49 (2018) 294–302.
[17] Y. Song, Y. Fu, S. Huang, L. Liao, Q. Wu, Y. Wang, F. Ge, B. Fang, Identification and antioxidant activity of bovine bone collagen-derived novel peptides prepared by recombinant collagenase from Bacillus cereus, Food Chem. 349 (2021), 129143.
[18] C. Zhou, J. Hu, X. Yu, A.E.A. Yagoub, Y. Zhang, H. Ma, X. Gao, P.N.Y. Otu, Heat and/or ultrasound pretreatments motivated enzymolysis of corn gluten meal: Hydrolysis kinetics and protein structure, LWT 77 (2017) 488–496.
[19] J. Borawska, M. Darewicz, G.E. Vegarud, P. Minkiewicz, Antioxidant properties of carp (Cyprinus carpio L.) protein ex vivo and in vitro hydrolysates, Food Chem. 194 (2016) 770–779.
[20] D.-H. Ngo, Z.-J. Qian, B. Ryu, J.W. Park, S.-K. Kim, In vitro antioxidant activity of a peptide isolated from Nile tilapia (Oreochromis niloticus) scale gelatin in free radical-mediated oxidative systems, J. Funct. Foods 2 (2010) 107–117.
[21] Y. Zhang, X. Ding, M. Li, Preparation, characterization and in vitro stability of iron-chelating peptides from mung beans, Food Chem. 349 (2021).
[22] Y. Zou, W. Wang, Q. Li, Y. Chen, D. Zheng, Y. Zou, M. Zhang, T. Zhao, G. Mao, W. Feng, X. Wu, L. Yang, Physicochemical, functional properties and antioxidant activities of porcine cerebral hydrolysate peptides produced by ultrasound processing, Process. Biochem. 51 (2016) 431–443.
[23] M.d.L.L.R. Menezes, H.L. Ribeiro, F.d.O.M.d.S. Abreu, J.P.d.A. Feitosa, M.d.S.M.d. S. Filho, Optimization of the collagen extraction from Nile tilapia skin (Oreochromis niloticus) and its hydrogel with hyaluronic acid, Colloids Surf. B 189 (2020), 110852.
[24] G. Liu, D. Wei, H. Wang, Y. Hu, Y. Jiang, Self-assembly of zein microspheres with controllable particle size and narrow distribution using a novel built-in ultrasonic dialysis process, Chem. Eng. J. 284 (2016) 1094–1105.
[25] F. Casanova, M.A. Mohammadifar, M. Jahromi, H.O. Petersen, J.J. Sloth, K. L. Eybye, S. Kobbelgaard, G. Jakobsen, F. Jessen, Physico-chemical, structural and techno-functional properties of gelatin from saithe (Pollachius virens) skin, Int. J. Biol. Macromol. 156 (2020) 918–927.
[26] Z. Song, H. Liu, L. Chen, L. Chen, C. Zhou, P. Hong, C. Deng, Characterization and comparison of collagen extracted from the skin of the Nile tilapia by fermentation and chemical pretreatment, Food Chem. 340 (2021), 128139.
[27] X. Zhao, T. Xing, X. Xu, G. Zhou, Influence of extreme alkaline pH induced unfolding and aggregation on PSE-like chicken protein edible film formation, Food Chem. 319 (2020), 126574.
[28] L. Sha, A.O. Koosis, Q. Wang, A.D. True, Y.L. Xiong, Interfacial dilatational and emulsifying properties of ultrasound-treated pea protein, Food Chem. 350 (2021), 129271.
[29] S.-Q. Tang, Q.-H. Du, Z. Fu, Ultrasonic treatment on physicochemical properties of water-soluble protein from Moringa oleifera seed, Ultrason. Sonochem. 71 (2021), 105357.
[30] T. Li, L. Wang, X. Zhang, H. Geng, W. Xue, Z. Chen, Assembly behavior, structural characterization and rheological properties of legume proteins based amyloid fibrils, Food Hydrocolloids 111 (2021), 106396.
[31] A.R. Vidal, R.L. Cansian, R.d.O. Mello, E.H. Kubota, I.M. Demiate, A.A.F. Zielinski, R.C.P. Dornelles, Effect of ultrasound on the functional and structural properties of hydrolysates of different bovine collagens, Food Sci. Technol. 40 (2020) 346–353.

[32] J. Pagan, A. Ibarz, V. Falguera, R. Benitez, Enzymatic hydrolysis kinetics and nitrogen recovery in the protein hydrolysate production from pig bones, J. Food Eng. 119 (2013) 655–659.
[33] X. Yang, L. Wang, F. Zhang, H. Ma, Effects of multi-mode S-type ultrasound pretreatment on the preparation of ACE inhibitory peptide from rice protein, Food Chem. 331 (2020), 127216.
[34] N. Rajapakse, E. Mendis, W.-K. Jung, J.-Y. Je, S.-K. Kim, Purification of a radical scavenging peptide from fermented mussel sauce and its antioxidant properties, Food Res. Int. 38 (2005) 175–182.
[35] S. Kangsanant, M. Murkovic, C. Thongraung, Antioxidant and nitric oxide inhibitory activities of tilapia (Oreochromis niloticus) protein hydrolysate: effect of ultrasonic pretreatment and ultrasonic-assisted enzymatic hydrolysis, Int. J. Food Sci. Technol. 49 (2014) 1932–1938.
[36] J. Zhao, J. He, Y. Dang, J. Cao, D. Pan, Ultrasound treatment on the structure of goose liver proteins and antioxidant activities of its enzymatic hydrolysate, J. Food Biochem. 44 (2019).
[37] W. Zhang, L. Huang, W. Chen, J. Wang, S. Wang, Influence of ultrasound-assisted ionic liquid pretreatments on the functional properties of soy protein hydrolysates, Ultrason. Sonochem. 73 (2021), 105546.
[38] C. Wen, J. Zhang, J. Zhou, M. Cai, Y. Duan, H. Zhang, H. Ma, Antioxidant activity of arrowhead protein hydrolysates produced by a novel multi-frequency S-type ultrasound-assisted enzymolysis, Nat. Prod. Res. (2019) 1–4.
[39] P. Fathi, M. Moosavi-Nasab, A. Mirzapour-Kouhdasht, M. Khalesi, Generation of hydrolysates from rice bran proteins using a combined ultrasonication-alcalase hydrolysis treatment, Food Biosci. 42 (2021), 101110.
[40] S. Karnjanapratum, S. Benjakul, Asian bullfrog (Rana tigerina) skin gelatin extracted by ultrasound-assisted process: characteristics and in-vitro cytotoxicity, Int. J. Biol. Macromol. 148 (2020) 391–400.
[41] S. Zhu, Q. Yuan, M. Yang, J. You, T. Yin, Z. Gu, Y. Hu, S. Xiong, A quantitative comparable study on multi-hierarchy conformation of acid and pepsin-solubilized collagens from the skin of grass carp (Ctenopharyngodon idella), Mater. Sci. Eng. C 96 (2019) 446–457.
[42] Y. Zou, H. Yang, P.P. Li, M.H. Zhang, X.X. Zhang, W.M. Xu, D.Y. Wang, Effect of different time of ultrasound treatment on physicochemical, thermal, and antioxidant properties of chicken plasma protein, Poult. Sci. 98 (2019) 1925–1933.
[43] H.B. Wijayanti, N. Bansal, H.C. Deeth, Stability of whey proteins during thermal processing: a review, Compr. Rev. Food Sci. Food Saf. 13 (2014) 1235–1251.
[44] S.M.T. Gharibzahedi, B. Smith, The functional modification of legume proteins by ultrasonication: a review, Trends Food Sci. Technol. 98 (2020) 107–116.
[45] X. Fan, S. Li, A. Zhang, H. Chang, X. Zhao, Y. Lin, Z. Feng, Mechanism of change of the physicochemical characteristics, gelation process, water state, and microstructure of okara tofu analogues induced by high-intensity ultrasound treatment, Food Hydrocolloids 111 (2021).
[46] Q. Cui, A. Zhang, R. Li, X. Wang, L. Sun, L. Jiang, Ultrasonic treatment affects emulsifying properties and molecular flexibility of soybean protein isolate-glucose conjugates, Food Biosci. 38 (2020).
[47] X. Shen, S. Shao, M. Guo, Ultrasound-induced changes in physical and functional properties of whey proteins, Int. J. Food Sci. Technol. 52 (2017) 381–388.
[48] A.N. Akram, C. Zhang, Extraction of collagen-II with pepsin and ultrasound treatment from chicken sternal cartilage; physicochemical and functional properties, Ultrason. Sonochem. 64 (2020).
[49] H. Zou, N. Zhao, S. Sun, X. Dong, C. Yu, High-intensity ultrasonication treatment improved physicochemical and functional properties of mussel sarcoplasmic proteins and enhanced the stability of oil-in-water emulsion, Colloids Surf. A 589 (2020).
[50] A.C. Karaca, N. Low, M. Nickerson, Emulsifying properties of chickpea, faba bean, lentil and pea proteins produced by isoelectric precipitation and salt extraction, Food Res. Int. 44 (2011) 2742–2750.
[51] S. Maqsood, A. Al-Dowaila, P. Mudgil, H. Kamal, B. Jobe, H.M. Hassan, Comparative characterization of protein and lipid fractions from camel and cow milk, their functionality, antioxidant and antihypertensive properties upon simulated gastro-intestinal digestion, Food Chem. 279 (2019) 328–338.
[52] Y. Li, Q.-H. Zeng, G. Liu, Z. Peng, Y. Wang, Y. Zhu, H. Liu, Y. Zhao, J.J. Wang, Effects of ultrasound-assisted basic electrolyzed water (BEW) extraction on structural and functional properties of Antarctic krill (Euphausia superba) proteins, Ultrason. Sonochem. 71 (2021).
[53] N.A. Mir, C.S. Riar, S. Singh, Physicochemical, molecular and thermal properties of high-intensity ultrasound (HIUS) treated protein isolates from album (Chenopodium album) seed, Food Hydrocolloids 96 (2019) 433–441.
[54] T. Xiong, W. Xiong, M. Ge, J. Xia, B. Li, Y. Chen, Effect of high intensity ultrasound on structure and foaming properties of pea protein isolate, Food Res. Int. 109 (2018) 260–267.
[55] F. Nasrollahzadeh, M. Varidi, M. Koocheki, F. Hadizadeh, Effect of microwave and conventional heating on structural, functional and antioxidant properties of bovine serum albumin-maltodextrin conjugates through Maillard reaction, Food Res. Int. 100 (2017) 289–297.